A new algorithm to discriminate internal fault current and inrush current utilizing feature of fundamental current

Nouvel algorithme utilisant la caractéristique du courant fondamental pour discriminer le courant de défaut interne et le courant d'appel

Jing Ma, Zengping Wang, Shuxia Zheng, Tong Wang, and Qixun Yang *

This paper presents a novel method to identify inrush current and internal fault current using the two-instantaneous-value-product algorithm to extract the variation feature of the fundamental current amplitude. First, the two-instantaneous-value-product algorithm is developed, and different variation trends of the fundamental current amplitude for inrush current and internal fault current are analyzed. Then, according to the descending features of the fundamental current amplitude, the inrush current and internal fault current can be distinguished from each other. A total of 216 experimental measurements have been tested on an YNd11 connected transformer. Dynamic testing results indicate that this method is able to clear internal faults, even light ones, within a cycle and is not affected by the current transformer saturation. Moreover, compared with the second harmonic restraint principle and the waveform comparison principle, the proposed algorithm has better performance. The computational simplicity of the proposed scheme enables its implementation in real-time applications with low-cost microprocessors.

Cet article présente une nouvelle méthode d'identification du courant d'appel et du courant de défaut interne. Dans cette méthode, l'algorithme « produit de deux valeurs instantanée » est utilisée pour déterminer la caractéristique de variation de l'amplitude du courant fondamental. En premier lieu, l'algorithme « produit de deux valeurs instantanée » est développé, ensuite, diverses tendances de variation de l'amplitude de la composante fondamentale du courant d'appel et du courant de défaut interne sont analysées. Se référant aux caractéristiques décroissantes de l'amplitude du courant fondamental, le courant d'appel et le courant de défaut interne peuvent être distingués l'un de l'autre. 216 mesures expérimentales ont été testées sur un transformateur connecté YNd11. Les résultats de tests dynamiques indiquent que cette méthode est capable de corriger les défauts internes, même les plus grands, pendant un cycle et n'est pas affectée par le courant de saturation du transformateur. De plus, comparé au deuxième principe de contrainte harmonique et au principe de comparaison de forme d'onde, l'algorithme proposé offre une meilleure performance. La simplicité du schéma proposé permet son implémentation, via des microprocesseurs bon marché, dans des applications temps réel.

Keywords: Transformer protection, two-instantaneous-value-product algorithm, fundamental current amplitude, inrush current, internal fault

I Introduction

With more and more large capacity transformers put into operation, the speed and reliability of transformer differential protection is often severely challenged [1]. The inrush current is one of the key factors leading to the mal-operation of differential protection. Therefore, distinguishing inrush current from the fault current is of significant value in the study of transformer differential protection. Principles currently in use for engineering include the second harmonic restraint principle, the waveform comparison principle, and the dead-angle principle. Among them the second harmonic restraint principle is mostly widely used [2]. However, with the improvement of the ferromagnetic material in modern large-capacity transformers, as well as the impact from the parallel capacitors and distributed capacitance of the UHV long distance transmission lines, the mal-operation rate of transformer protection schemes based on the second harmonic restraint principle is greatly increased [3]. As for the waveform comparison principle and the dead-angle principle, both work by directly or indirectly utilizing the intermittent feature of the inrush current.

In protection settings based on these two principles, the symmetry angle and lock angle are difficult to choose and can only be set and modified by real-time tests, which bear the hidden problem of mal-operation. Therefore, some other differential current-based techniques have been adopted in differential protection. These techniques include fuzzy logic [4]-[6], waveform correlation [7], wavelet analysis [8]-[12], and artificial neural network [13]-[16]. These techniques provide alternatives or improvements to the existing protective relaying functions. However, they may require large data storage for training or comparing, large computational burden, large memory to accommodate the required algorithms, and/or dependence on the transformer parameters. Thus, there exists a need to present a practical power transformer protection, which is able to identify inrush currents rapidly and be tested without the need of transformer parameters.

Manuscript received January 6, 2013; accepted February 8, 2013.

* Jing Ma is with the School of Electrical and Electronic Engineering, North China Electric Power University, Changping, Beijing, P. R. China, and also with the Bradley Department of Electrical and Computer Engineering, Virginia Polytechnic Institute and State University, Blacksburg, Virginia, USA.

Zengping Wang, Shuxia Zheng, Tong Wang, and Qixun Yang are with the School of Electrical and Electronic Engineering, North China Electric Power University, Changping, Beijing, P. R. China.

This work was supported by The National Basic Research Program of China (973 Program) (2012CB215200); National Natural Science Foundation of China (50907021, 50837002); The"111"Project (B08013); The Chinese University Scientific Fund Project (11MG01, 09QX64); The Project Sponsored by the Scientific Research Foundation for the Returned Overseas Chinese Scholars, State Education Ministry ([2011] No. 1139); Hebei Natural Science Foundation (E2012502034); Electric Power Youth Science and Technology Creativity Foundation of CSEE ([2012] No. 46).

Associate Editor managing this paper's review: A. Khajehoddin

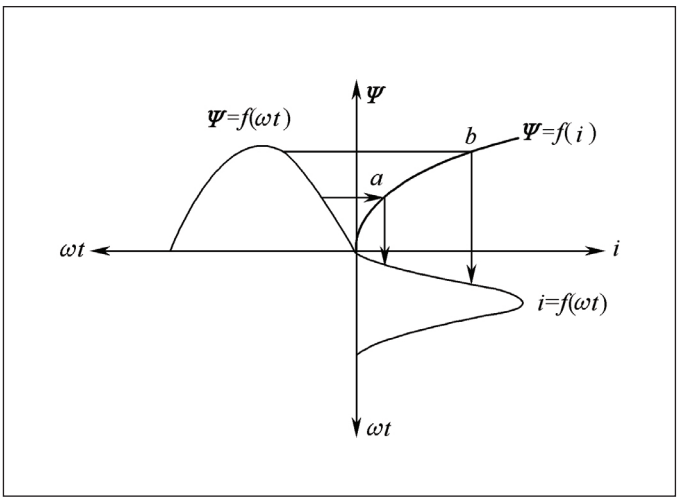

Figure 1: *Waveform of inrush current*

In fact, apart from being intermittent, the inrush current is also different from the internal fault current in waveform in other aspects [17, 18]. Thorough study of the formation mechanism of the transformer inrush current reveals that, due to the nonlinearity of the magnetization curve of the transformer magnetic conductor, the inrush current waveform will be greatly distorted (in a concave manner) where the magnet core enters and exits from saturation. Thus, by applying the two-instantaneous-value-product algorithm, the calculated fundamental amplitude of the inrush current will manifest acute changes in value. As for the fault current, since it is basically sinusoidal, the fundamental amplitude changes in a relatively modest way except at the point where the fault occurs.

The two-instantaneous-value-product algorithm is used to calculate the real-time fundamental current amplitude in different cases, and then according to different variation features of the amplitude, the protection criterion is proposed in this paper. Dynamic testing results show that this method has the advantages of simple computation, rapid distinguishing and high sensitivity. Moreover, compared with the second harmonic restraint principle and the waveform comparison principle, the proposed algorithm has better performance.

II Basic principles

II.A The two-instantaneous-value-product algorithm

Suppose

$$\begin{cases} i_{t1} = I_{\mathrm{m}} \sin \omega t_1 \\ i_{t2} = I_{\mathrm{m}} \sin \omega t_2 = I_{\mathrm{m}} \sin \omega (t_1 + T_s) \end{cases} \tag{1}$$

where t_1 is the current sampling point and t_2 is the next sampling point. T_{s} is the time interval between two sampling points, i.e. $T_{\mathrm{s}}=t_2-t_1$.

Applying the two-instantaneous-value-product algorithm [19], the fundamental current amplitude is

$$I_{\mathrm{m}} = \sqrt{\frac{i_{t1}^2 + i_{t2}^2 - 2 i_{t1} i_{t2} \cos \omega T_{\mathrm{s}}}{\sin^2 \omega T_{\mathrm{s}}}} \tag{2}$$

II.B Characteristic of the inrush current fundamental amplitude

When the transformer is no-load closed, the inrush current waveform is greatly distorted (in a concave manner) where the magnet core enters and exits from saturation, as shown in Fig. 1 [20].

A total of 56 cases were carried out in this situation. The inrush current waveform is a function of the different core residual magnetization and the switching instant, so the inrush current waveforms are different from each other. In Fig. 2, the differential current waveforms of the

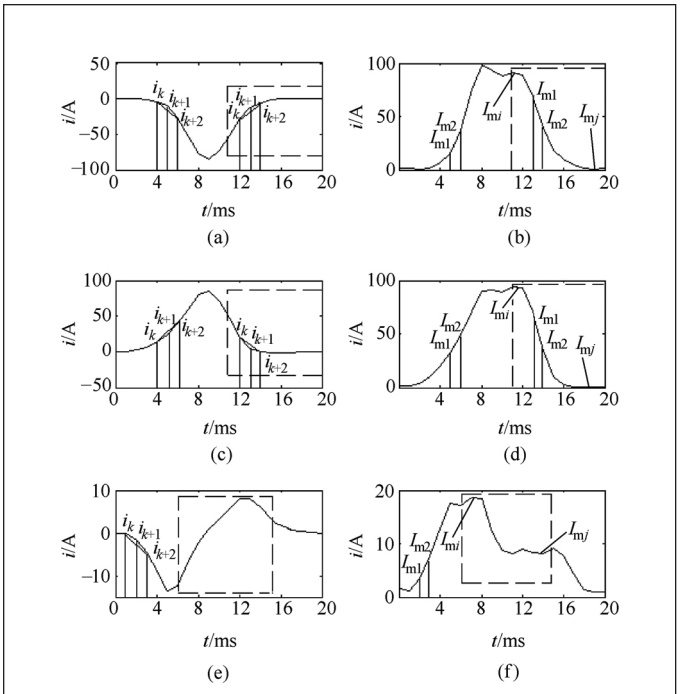

Figure 2: *Inrush currents and their fundamental current amplitudes*

transformer no-load closed under different conditions in the dynamic testing system and the corresponding fundamental current amplitude variation curves are displayed. The asymmetric inrush current on the lower half plane, as well as the asymmetric and symmetrical inrush currents on the upper half plane are shown in Figs. 2(a), 2(c), and 2(e) respectively.

Choose any three adjacent sampling points i_k, i_{k+1}, and i_{k+2} in the magnet core saturation area. Applying (2), the fundamental current amplitudes I_{m1} and I_{m2}, which are based on i_k and i_{k+1}; i_{k+1} and i_{k+2} respectively can be gained. The quadratic difference between I_{m1} and I_{m2} is:

$$\begin{aligned} I_{\mathrm{m2}}^2 - I_{\mathrm{m1}}^2 &= \left[(i_{k+2}^2 + i_{k+1}^2 - 2 i_{k+2} i_{k+1} \cos \omega T_{\mathrm{s}}) - \right. \\ &\qquad \left. \frac{i_{k+1}^2 + i_k^2 - 2 i_{k+1} i_k \cos \omega T_{\mathrm{s}}}{\sin^2 \omega T_{\mathrm{s}}} \right] \\ &= (i_{k+2} - i_k) \frac{[i_{k+2} + i_k - 2 i_{k+1} \cos \omega T_{\mathrm{s}}]}{\sin^2 \omega T_{\mathrm{s}}} \end{aligned} \tag{3}$$

When the initial current is the asymmetric inrush current on the lower half plane, as shown in Fig. 2(a), according to the concave characteristic of the inrush current, (4) can be found to be

$$\frac{i_{k+2} - 2 i_{k+1} \cos \omega T_{\mathrm{s}} + i_k}{T_{\mathrm{s}}^2} < \frac{i_{k+2} - 2 i_{k+1} + i_k}{T_{\mathrm{s}}^2} < 0 \tag{4}$$

In the meantime, the descending degree of the inrush current i_{k+2}-i_k<0, and the ascending degree i_{k+2}-i_k>0. According to (3), when the magnet core enters the saturation area (the descending session of the waveform), $I_{\mathrm{m2}}>I_{\mathrm{m1}}$, and the fundamental current amplitude keeps increasing monotonously; while when the magnet core exits from saturation (the ascending session of the waveform), $I_{\mathrm{m2}}<I_{\mathrm{m1}}$, and the fundamental current amplitude keeps decreasing monotonously.

When the initial current is the asymmetric inrush current on the upper half plane, as shown in Fig. 2(c), in the vicinity of the saturation area we have

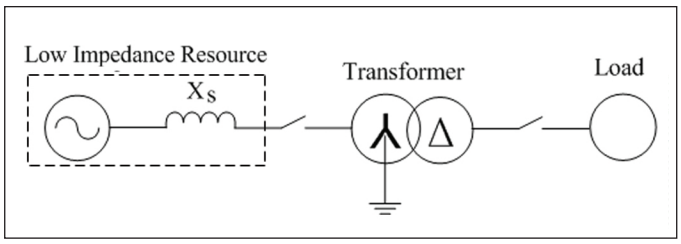

Figure 3: *Connection scheme of the dynamic analog testing system*

$$\frac{i_{k+2}-2i_{k+1}\cos\omega T_s+i_k}{T_s^2} > \frac{i_{k+2}-2i_{k+1}+i_k}{T_s^2} > 0 \qquad (5)$$

In the meantime, the ascending degree of the inrush current i_{k+2}-i_k>0, and the descending degree i_{k+2}-i_k<0. According to (3), when the magnet core enters the saturation area (the ascending section of the waveform), $I_{m2}>I_{m1}$, and the fundamental current amplitude keeps increasing monotonously. When the magnet core exits from saturation (the descending section of the waveform), $I_{m2}<I_{m1}$, the fundamental current amplitude keeps decreasing monotonously.

It should be noted that after the magnet core enters the deep saturation area (i.e. the linear part of the ferromagnetic curve), the inrush current waveform will be sinusoidal, which means the fundamental current amplitude will be steady thereafter.

The testing results of the fundamental current amplitude under the conditions given in Figs. 2(a) and (c) are shown in Figs. 2(b) and (d) respectively. Obviously, the variation trends of the fundamental current amplitude are consistent with the theoretical analysis above.

The waveforms of symmetrical inrush currents and the corresponding fundamental current amplitude curves are shown in Figs. 2(e) and (f) respectively. Similarly, it can be concluded that the fundamental amplitude tends to ascend when the magnet core enters saturation and descend when the magnet core exits from saturation.

II.C Characteristic of the fundamental current amplitude when no-load closing at an internal fault

When taking into account the transformer winding resistance, the hyseresis loss, and the eddy current loss, the loop voltage equation of the transformer based on the equivalent instantaneous inductance [9] can be set as:

$$u_1 = r_k i_d + L_k \frac{di_d}{dt} \qquad (6)$$

where i_d is the current difference between the primary side and the secondary side; r_k is the equivalent resistance; L_k is the equivalent instantaneous inductance; u_1 is the terminal voltage of the primary side.

Consider that transformers are usually highly inductive, especially large-capacity power transformers, whose equivalent resistance is very small. Thus, the first item in (6) is much smaller than the second item. Neglecting the first item, the differential expression of i_d can be obtained:

$$\frac{di_d}{dt} \approx \frac{u_1}{L_k} \qquad (7)$$

According to (7), the waveform characteristic of i_d is decided by the ratio of the primary side terminal voltage to the equivalent instantaneous inductance. The primary side terminal voltage u_1 mutates only when an internal fault occurs (whether the transformer is loaded or not), and u_1 keeps steady when the transformer operates in the normal state or in the post-fault steady state. Therefore, on the basis of a whole current cycle, it is the instantaneous inductance L_k that really counts. When an internal fault occurs to the transformer, the magnet core is no longer saturated, so that the excitation inductance and leakage inductance are constant. Thus, the instantaneous inductance L_k is also constant. Therefore, the waveform of the current difference i_d remains sinusoidal except for the fault point. The fundamental current amplitude calculated using the two-instantaneous-value-product algorithm is supposed to remain the same in this area.

III Protection scheme design

According to the analysis above, the difference between the inrush current and fault current lies in the descending degree of the fundamental current amplitude during the magnet core's exit from saturation. Based on this conclusion, a new identification criterion is proposed in this paper as follows.

(a) Identify the current bias direction.

Determine the maximum and minimum values of the current i_{max} and i_{min} within half a cycle of data window after the transformer is no-load closed. If $|i_{max}|$-$|i_{min}| \geq 0$,then the current is forward-biased; otherwise, if $|i_{max}|$-$|i_{min}| < 0$, then the current is reverse-biased.

(b) Identify the exit-saturation area of the transformer magnet core.

Starting from half a cycle after the transformer's no-load closing, summarize the sampling points of each cycle to form curve S_k. For forward-biased current, the sampling sequence corresponding to the minimum positive value on the descending session of curve S_k is chosen to be the exit-saturation area (see the dashed line frame in Fig. 2(c)). For reverse-biased current, the sampling sequence corresponding to the maximum negative value on the ascending session of curve S_k is chosen to be the exit-saturation area (see the dashed line frames in Figs. 2(a) and (e)). After the exit-saturation area is decided, take the maximum and minimum values of the fundamental current amplitude in this area as I_{mi} and I_{mj}, as shown in Figs. 2(b), (d) and (f).

(c) Calculate the changing rate of the fundamental current amplitude k according to (8).

$$k = \left| \frac{I_{mi} - I_{mj}}{I_{mj}} \right| \qquad (8)$$

If $k \geq k_{set}$ (k_{set} is the setting value), then it can be decided to be the inrush current, thus the differential protection should be locked; otherwise, if $k < k_{set}$ and the starting requirement is also met, then the internal fault is decided and relay protection should operate to trip.

IV Simulation verification

To verify the effectiveness of the proposed method, experimental tests [21-23] have been carried out at the Electrical Power Dynamic Laboratory (EPDL).

IV.A The dynamic testing system

The experimental transformer is a three-phase, two-winding transformer bank with YNd11 connection, which is fed by a low impedance source, as shown in Fig. 3. The parameters of the two-winding transformers are given in Table I. Three identical current transformers (CTs) are connected in Δ on the primary side, and another three identical CTs are connected in Y on the secondary side of the power transformer.

The experiments provide different switching and clearing instants for inrush currents, as well as different faults and different numbers of turns for internal faults. A total of 216 cases have been tested and divided into five main categories: 56 cases for switching the transformer with no load, 52 cases for simultaneous internal fault and inrush conditions, 54 cases for faulty conditions only, and 54 cases for external faults with the CT in saturation conditions, to test the algorithm.

Table 1

Parameters of each single phase unit of transformer used in the test

Rated power	10kVA
Rated voltage ratio	1000/380V
Rated frequency	50Hz
No load current	1.45%
No load loss	1%
Short circuit voltage	9.0~15.0%
Short circuit loss	0.35%

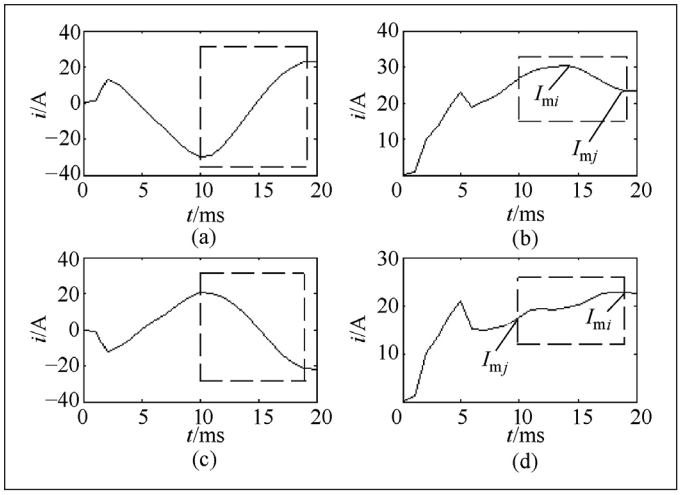

Figure 4: *Current waveforms and their fundamental current amplitudes when switching in transformer with an internal turn-turn fault*

IV.B Testing result analysis

The switching in the transformer bank with no load often causes the inrush current of nonfault phases, which has been verified by a total of 52 cases with simultaneous inrush currents and internal faults. An example taken from these cases is given in Fig. 4, where the no-load transformer closes at a phase A 3.6% (turn ratio) turn-to-turn fault. The waveforms of the fault phase differential current are shown in Figs. 4(a) and (c), respectively. And their fundamental current amplitudes are shown in Figs. 4(b) and (d), respectively. From Figs. 4(a) and (c), it can be seen that, in the first half cycle, the differential current manifests obvious inrush current features; while in the second half cycle, as the magnet core exits from saturation, the differential current displays the characteristic of fault current. According to the identification criterion proposed above, the fundamental current amplitudes in the exit-saturation area corresponding to the differential currents in Figs. 4(a) and (c) are calculated and shown in Figs. 4(b) and (d) respectively (the dashed line frame). Applying (8), the changing rates of the fundamental current amplitudes are gained, i.e. k_b=0.27, k_d=0.25.

Data from a total of 54 cases are used to test the algorithm under faulty conditions. An example taken from these cases is given in Fig. 5, where a phase A 3.6% turn-to-turn fault occurs in the loaded transformer. The waveforms of the fault phase differential current are shown in Figs. 5(a) and (c), respectively. And their fundamental current amplitudes are shown in Figs. 5(b) and (d), respectively. From Figs. 5(b) and (d), it can be seen that, for either forward-biased or reverse-biased current, the fundamental current amplitude remains constant in the exit-saturation area. Applying the identification criterion, the changing rates of the fundamental current amplitudes in Figs. 5(b) and (d) can be calculated, i.e. k_b=0.14, k_d=0.13.

The experiments provide different switching and clearing instants

Table 2

Calculation results of k under different operation states of two-winding transformer

Operation state				k	Testing number
No-load closing				1.435～87.84	1
Faults at Y-side	Closing at faults	Turn ratio	A3.6%	0.23～0.32	2
			A6.1%	0.05～0.12	3
			A9.0%	0.04～0.11	4
			B18%	0.03～0.05	5
			C18%	0.03～0.06	6
		Phase to ground	A	0.02～0.04	7
			B	0.03～0.05	8
	Faults occuring when transformer loaded	Turn to turn	A3.6%	0.11～0.14	9
			A6.1%	0.05～0.09	10
			A9%	0.04～0.06	11
			B18%	0.02～0.03	12
			C18%	0.03～0.05	13
		Phase to ground	A	0.01～0.03	14
			B	0.01～0.02	15
No-load closing at△-side			A4.5%	0.18～0.29	16
Faults at △- side			A4.5%	0.10～0.19	17

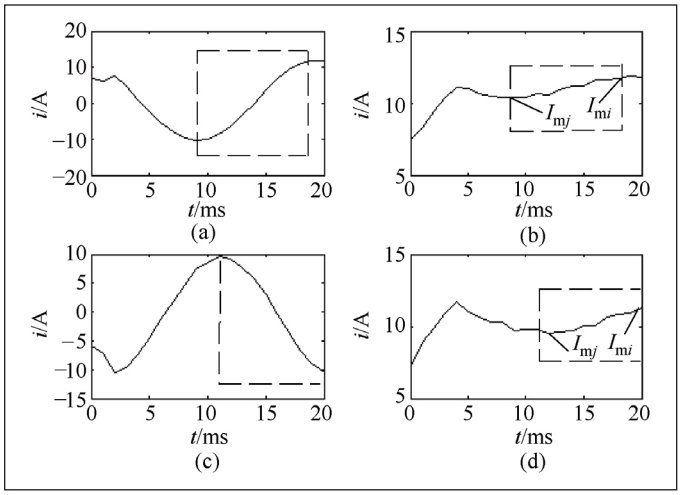

Figure 5: *Current waveforms and their fundamental current amplitudes when an internal turn-to-turn fault occurs*

for inrush currents, as well as a different faults and different number of turns for internal faults. The changing rates of the fundamental current amplitude k gained under different operation states of the transformer are shown in Table II. In the case of inrush currents, the changing rate of the fundamental current amplitude for each phase is calculated; while in the case of fault currents (including faults at no-load closing),

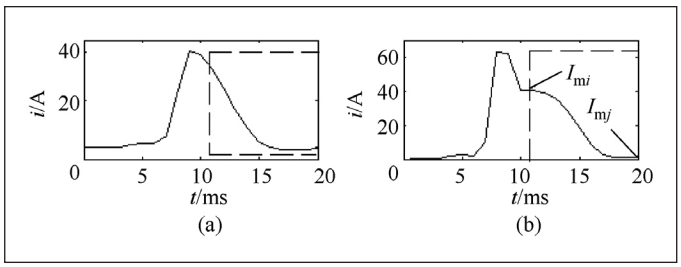

Figure 6: *Current waveforms and its fundamental current amplitudes under TA saturation at out-zone fault*

only the fault phase is analyzed. It can be seen from Table II that, the minimum value of k for inrush currents is 1.435, while the maximum value of k for internal faults is 0.32. The changing rates being more than four times apart, by properly setting the threshold value, the distinguishing between inrush currents and fault currents can be reliably done.

With the same testing data, the calculation results using the second harmonic restraint principle and the waveform comparison principle are shown in Table III. For the waveform comparison principle, the waveform coefficient of the differential current is displayed. In the case of no-load closing, the waveform coefficients of all three phases are given, while in the case of no-load closing at faults, only the maximum coefficient of the three phases is given. For the second harmonic restraint principle, the percentage of the second harmonic component in the fundamental component of the differential current is displayed. In the case of no-load closing, the second harmonic percentage of all three phases is given, while in the case of no-load closing at faults, only the minimum percentage of the three phases is given.

For the waveform comparison principle, when the phase constraint method is used with the threshold value set to be 0.5, some testing data (the *-marked ones) can not be clearly identified, as shown in Table III. For example, in the cases of no-load closing at internal turn-to-turn faults (including turn-to-turn faults on the Y-side with turn radio 3.6%, 6.1% and 9%), since none of the three phase current waveform coefficients exceeds 0.5, relay protection will operate with a long time delay. For the second harmonic restraint principle, if the threshold value is set to be 15%, operation of the protective relay will also be delayed when the transformer closes with no-load at certain internal turn-to-turn faults.

Comparing Table II and Table III, it is obvious that the proposed new principle has better performance than the second harmonic restraint principle and the waveform comparison principle in identifying the inrush current. This is mainly due to the application of the two-instantaneous-value-product algorithm in the new principle, which facilitates its localization capability of dynamically portaiting the spatial distribution of the fundamental current amplitude.

IV.C TA saturation caused by external faults

The differential current is designed to restrain under normal load flows and for external faults. However, if the TAs saturate, external short circuits can in fact result in very large differential currents, which has been proved by a total of 54 cases. Therefore, the way TV saturation influences the protection criterion when there is an external fault is studied in this paper. In the transient after the external fault occurs, the short circuit current contains a big dc component. Since TA transforms dc components with a large error, a rapid TA saturation will result, which then causes the induced electromotive force on the secondary winding to drop to zero immediately, and the current on the secondary winding remains zero in the same period. With the current on the primary winding decreased, TA will exit from saturation, thus the induced electromotive force and current on the secondary winding will increase accordingly.

It can be concluded that, as TA enters and exits from saturation, the differential current on the secondary winding will experience severe distortion (in the manner of a concave) in the waveform. In accordance with the distortion parts, the fundamental current amplitude will also experience severe distortion, as shown in Fig. 6. And the changing rate of the fundamental current amplitude in this case is calculated to be k=35.72. Analysis of TA saturation under different types of external faults shows that, the protection principle based on the changing rate of the fundamental current amplitude is reliable in locking the differential protection.

Table 3

Dynamic simulation results of wave comparison and second harmonic restrain algorithm

Operation state				waveform comparison principle	second harmonic restraint principle (%)
No-load closing				0.014～0.451	15.30～72.69
Faults at Y-side	Closing at faults	Turn to turn	A3.6%	0.286～0.374*	29.57～38.65*
			A6.1%	0.428～1.107*	8.58～15.79*
			A9%	0.349～0.887*	8.17～13.56
			B18%	0.641～1.080	5.54～9.52
			C18%	0.655～1.143	3.81～10.34
		Phase to ground	A	0.609～1.058	2.16～3.95
			B	0.627～1.106	2.55～3.36
No-load closing at△-side			A4.5%	0.860～1.115	9.68～12.97

*P.S. The *–marked data indicate the cases that can not be clearly identified with the waveform comparison or the second harmonic restraint principle.*

V Conclusion

A novel method to rapidly indentify inrush current and the internal fault current based on the changing rate of the fundamental current amplitude is proposed in this paper. A large number of measurements were carried out to test the proposed method. The new principle has the following advantages.

1. Rapidity in identification (within a cycle).
2. Universality in application to different types of transformers.
3. Higher reliability and sensitivity than traditional identification principles.
4. Reliability in locking the differential protection in TA saturation caused by external faults.

Acknowledgment

Many faculties and students contributed greatly to this research. The authors would like to thank Dr. Yilu Liu, Dr. James S. Thorp and Dr. Arun G. Phadke.

References

[1] A. G. Phadke and J. S. Thorp, "A new computer-based flux-restrained current-differential relay for power transformer protection," *IEEE Trans. Power Appl. Syst.*, vol. PAS-102, no. 11, pp. 3624–3629, Nov. 1983.

[2] P. Liu, O. P. Malik, C. Chen, G. S. Hope, and Y. Guo, "Improved operation of differential protection of power transformers for internal faults," *IEEE Trans. Power Delivery*, vol. 7, no. 4, pp. 1912–1919, Oct. 1992.

[3] R. S. Girgis and E. G. teNyenhuis, "Characteristics of inrush current of present designs of power transformer" in *Proc. IEEE Power Engineering Society General Meeting*, Tampa, Florida, USA, Jun. 24-28, 2007.

[4] A. Wiszinewski and B. Kasztenny, "A multi-criteria differential trans-former relay based on fuzzy logic," *IEEE Trans. Power Del.*, vol.10, no. 2, pp.1786-1792, Oct. 1995.

[5] A. Ferrero, S. Sangiovanni, and E. Zappitelli, "A fuzzy-set approach to fault-type identification in digital relaying," *IEEE Trans. Power Del.*, vol.10, no. 1, pp.169-175, Jan. 1995.

[6] B. Kasztenny, E. Rosolowski, M. M. Saha, and B. Hillstrom, "A self-organizing fuzzy logic based protective relay-an application to power transformer protection," *IEEE Trans. Power Del.*, vol.12, no. 3, pp.1119-1127, Jul. 1997.

[7] X.-N. Lin, P. Liu, and O. P. Malik, "Studies for identification of the inrush based on improved correlation algorithm," *IEEE Trans. Power Del.*, vol. 17, no. 4, pp. 901–907, Oct. 2002.

[8] M. G. Morante and D. W. Vicoletti, "A wavelet-based differential transformer protection," *IEEE Trans. Power Del.*, vol. 8, no. 4, pp. 1351–1358, Oct. 1993.

[9] S. K. Pandy and L. Satish, "Multiresolution signal decomposition: A new tool for fault detection in power transformers during impulse tests," *IEEE Trans. Power Del.*, vol. 13, no. 4, pp. 1194–1200, Oct. 1998.

[10] Y. Sheng and M. Steven, "Decision trees and wavelet analysis for power transformer protection," *IEEE Trans. Power Del.*, vol. 17, no. 2, pp. 429–433, Apr. 2002.

[11] O. A. S. Youssef, "A wavelet-based technique for discrimination between faults and inrush currents in transformers," *IEEE Trans. on Power Del.,* vol.18, no.1, pp.170-176, Jan. 2003.

[12] S. A. Saleh and M. A. Rahman, "Real-time testing of a WPT-based protection algorithm for three-phase power transformers," *IEEE Trans. Indus. Appl.*, vol. 41, no. 4, pp. 1125–1132, Jul. 2005.

[13] L. G. Perez, A. J. Flechsig, J. L. Meador, and Z. Obradoviic, "Training an artificial neural network to discriminate between magnetizing inrush and internal faults," *IEEE Trans. Power Del.*, vol. 9, no. 1, pp. 434–441, Jan. 1994.

[14] P. B. Grcar and D. Dolinar, "Improved operation of power transformer protection using artificial neural network," *IEEE Trans. Power Delivery*, vol. 12, no. 3, pp. 1128–1136, Jul. 1997.

[15] M. R. Zaman and M. A. Rahman, "Experimental testing of the artificial neural network based protection of power transformers," *IEEE Trans. Power Del.*, vol.13, no. 2, pp.510-517, Apr. 1998.

[16] Á. L. Orille-Fernández, N. K. I. Ghonaim, and J. A. Valencia, "A FIRANN as a differential relay for three phase power transformer protection," *IEEE Trans. Power Del.*, vol. 16, no. 2, pp. 215–218, Mar. 2001.

[17] Chen Deshu, Yin Xianggen, Zhang Zhe, et al, "Virtual third harmonic restrained transformer differential protection principle and practice," *Proceedings of the CSEE*, vol. 21, no. 8, pp. 19–23, Aug. 2001.

[18] Zhang Xuesong, He Benteng, "A new method to identify inrush current based on estimation," *Proceedings of the CSEE*, vol. 25, no. 3, pp. 94–99, Mar. 2005.

[19] Zhang Ju, "Principle of Protective Relaying Based on Microcomputers". *Water Conservancy and Hydropower Publishing House*, Beijing, China, 2004.

[20] Ye Dong, "Electro-mechanics," *Tianjin Science and Technology Publishing House*, Tianjin, China, 1994.

[21] Ma Jing, Wang Zengping, "Analysis of normalized grille curve in time and frequency domains to identify magnetizing inrush," *Transactions of China Electrotechnical Society*, vol. 27, no. 6, 78–81, Jun. 2007.

[22] Wang Zengping, Xu Yan, Wang Xue, et al, "Study on the novel transformer protection principle based on the transformer model," *Proceedings of the CSEE*, 2003, 23(12): 54-58, vol. 23, no. 12, pp. 54–58, Dec. 2003.

[23] Xu Yan, Wang Zengping, Yang Qixun, et al, "Research on novel transformer protection based on the charac- teristics of voltage and differential current," *Proceedings of the CSEE*, vol. 24, no. 2, pp. 61–65, Feb. 2004.

Jing Ma (S'06-M'08) was born in Hebei Province, China on February 25, 1981. He received his B.S. and Ph.D. degree from North China Electric Power University, China, in 2003 and 2008, respectively. He has been a visiting research scholar in the Bradley Department of Electrical and Computer Engineering, Virginia Polytechnic Institute and State University from 2008 to 2009. He is currently an associate professor in the School of Electrical and Electronic Engineering, North China Electric Power University, China. His major interests include power system equipment modeling, diagnoses and protection (e-mail: hdmajing@yahoo.com.cn).

Zengping Wang (M'05) was born in Hebei Province, China, on November 3, 1964. He received the B.S. and M.S. degree in Electric Engineering from North China Electric Power University, China, in 1985 and 1988, respectively. He received the Ph.D. degree from Harbin Institute of Technology, China, in 1997. He is a professor and the dean of the School of Electrical and Electronic Engineering at North China Electric Power University. His special fields of interest include power system equipment protection, fault analysis and wide-area protection (e-mail: wangzp1103@yahoo.com.cn).

Shuxia Zheng is currently a Masters student in the School of Electrical and Electronic Engineering, North China Electric Power University, China. She received her B.S. degree from North China Electric Power University in 2009. Her interests include power system adaptive protection and control. (e-mail: joerain717@ncepu.edu.cn).

Tong Wang is currently a Ph.D. candidate in the School of Electrical and Electronic Engineering, North China Electric Power University, China. She received her B.S degree from North China Electric Power University in 2007. Her interests include wide area measurements, and small signal analysis and control. (e-mail: hdwangtong@126.com).

Qixun Yang was born in Shanghai, China, on October 30, 1937. He received B.S. and Ph.D. degrees from Zhejiang University, China, and South Wales University, Australia, in 1960 and 1982 respectively. He is currently a Chinese academician of engineering and a professor of North China Electric Power University. He is also the Board Chairman of Beijing Sifang Automation Co., Ltd. His research interests include power system protection and control, and substation automation (e-mail: yangqixun@yahoo.com.cn).